Original Research Article

Experimental Evaluation of Double Air Pass Solar Collector in Humid Tropical Environment

ABSTRACT

The present work was focused on the experimental investigation of a double air pass solar collector which was designed and constructed at the Laboratory of Energetic and Thermal Applied of the National School of Agro-Industrial Sciences of the University of Ngaoundere. It consists of a double glazed cover with a surface of 0.47 m², an absorbent plate and a layer of thermal insulation. It allows simultaneous circulation and the same flow direction of the working fluid (air) on both side of the absorber. The experimental tests were conducted outdoor, in natural environment of Ngaoundéré city, during one month period, from 4 to 30 of April, between 9:00 am and 5:00 pm, local time. The research aim was to characterize, on one hand, the local weather conditions (solar radiation, ambient temperature, relative humidity and wind velocity), and on the other hand the collector performance. The solar collector was permanently oriented towards the South and tilted by 45° with respect to the horizontal plane. The analysis of the temperature profiles of different components of the collector showed that the maximum temperature was reached at 2:30 pm, when solar radiation was 1217 W/m² and they were 73.9 °C, 61.7 °C and 44.7 °C for absorber, inner glass and outer glass, respectively. As concerning the outlet temperature of the heat transfer fluid, the analysis of the results shows that it goes up to 58.4 °C and 52.2 °C, while thermal efficiency was as high as 47.81% and 65.57% when the air flow velocities were setup at 0.5 m/s and 1.5 m/s, respectively.

Key words: Solar collector, thermal performance, double pass, double glasses, experimental characterization.

1. INTRODUCTION

In everyday life, the heat is always necessary and indispensable. Heat can be used in domestic applications (Floride *et al.,* 2002), in industrial processes (Kalogirou, 1997), in drying processes (Fudholi and Sopian, 2019; Fouakeu *et al.,* 2019; Agbossou *et al.,* 2016; Mokhtari and Semmar, 2001) and in many others (Gorjian *et al.,* 2020; Suman *et al.,* 2015). Heat production can be achieved in many ways such as using electrical energy, fossil or renewable energy sources, primarily solar energy (Mahmut and Saffa, 2015), etc. Indeed, the solar radiation reaching the earth, i.e. $1.76*10^{17}$ W, is far greater than the global consumption needs (Dountio *et al.,* 2010). The radiant energy from the sun is generally converted either into electricity using photo voltaic panels or into thermal energy through solar collectors. The latter devices are designed to transform the radiant energy of the sun into thermal energy and to transmit it to a heat transfer fluid (Aoues *et al.,* 2009).

Several works have been carried out with a view to improve the efficiency of solar collectors. Most of these works have led to the design and construction of different configurations of flat-plate, single-glazed or double-glazed solar collectors.

Improvement of the performance of these systems is achieved, on one hand, by increasing the convection heat transfer coefficient between the absorber surface and the air by using an internal swirling flow (Hu *et al.,* 2020) and, on the other hand, by reducing heat losses through different components of the collector. However, performance Improvement can be done by increasing the heat exchange surface through artificial roughness techniques (Labed *et al.,* 2012; 2009; Ahmed-Zaid *et al.,* 1999).

In the study conducted by Ihaddadene *et al.* (2014) it has been shown that the thermal performance of the double-glazed collector is higher than that of a single-glazed collector. They have also shown that the efficiency of the double-glazed collector decreases as the distance between the two panes of glass increases. Similarly, Tetang and Ghiaus (2019) analyzed the effect of the distance between the absorber and the lower glass pane and between the absorber and the insulation. The results obtained from the simulation showed that the efficiency is maximum (approximately 50%) when the ratio of these two distances is equal to 1. At the same time, they have shown in their work that by varying the flow rate of the heat transfer fluid, the thermal efficiency also varies. Thus, when the air (heat transfer fluid) velocity increases; the instantaneous thermal efficiency of the collector also increases.

Therefore, the experimental characterization of a double air pass solar collector will be analyzed and discussed. It will precisely characterize the thermal behavior of the main components of the collector: the absorber, the inner glass, the outer glass and the heat transfer fluid at the inlet and at the outlet. The results will give the opportunity to other researchers to validate their numerical models and simulations of similar solar collectors.

2. MATERIALS AND METHODS

2.1 Experimental device and measuring instruments

A picture taken in situ with the experimental device is presented in Figure 1.

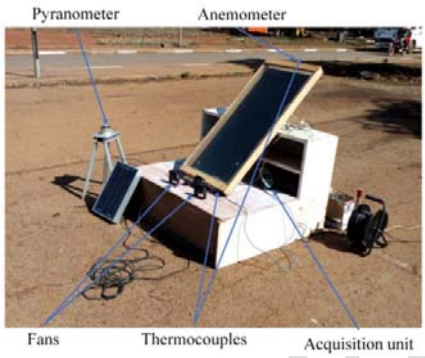

Fig. 1. Experimental device

A FLA613GS type pyranometer was used to measure the global solar irradiation, the air velocity was measured by a Almemo FVAD 15S120 R1E4 type propeller anemometer, the air humidity by a Almemo ZAD936 RAK type hygrometer, and the temperature in different locations by K type thermocouples using a "Almemo 2590" data acquisition unit with four inputs on which the thermocouples were mounted for displaying different temperature values during operation.

2.2 Experimental protocol

The tests were carried out during the period from April 4 to April 30, in the city of Ngaoundere (Latitude: 7.33°N; Longitude: 13.58°E; Altitude: 1205 m). The complete system was oriented to the South with an inclination of 45° with respect to the horizontal plane. Fluid circulation is imposed at constant velocity by means of three electrical fans (Model: AD0912US-A70GL). The measured parameters are read every 15 minutes between 9:00 am and 5:00 pm.

The characterization of the collector consisted, first of all, in recording the temperatures of the absorber, of the inner glass and of the outer glass of the solar thermal collector, according to the sunshine of the day, and afterwards to evaluate the instantaneous global efficiency.

Figure 2 shows the three different configurations that were studied.

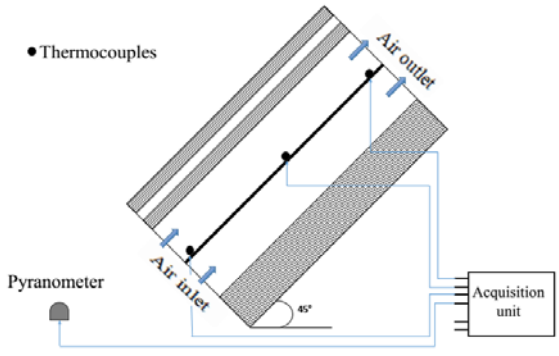

(a) Configuration for monitoring the temperature of the absorber

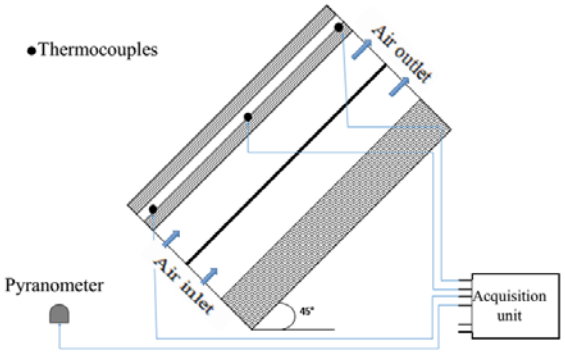

(b) Configuration for monitoring the temperature of the lower glass pane

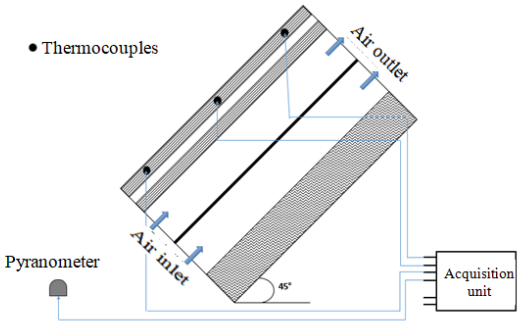

(c) Configuration for monitoring the temperature of the upper glass pane

Fig. 2. Configurations to measure the temperature of (a) the absorber (b) the inner glass pane (c) the outer glass pane

Figure 3 shows the configuration used to measure heat transfer fluid inlet/outlet temperatures for different air flow velocities. These parameters were used to evaluate the overall instantaneous performance of the collector.

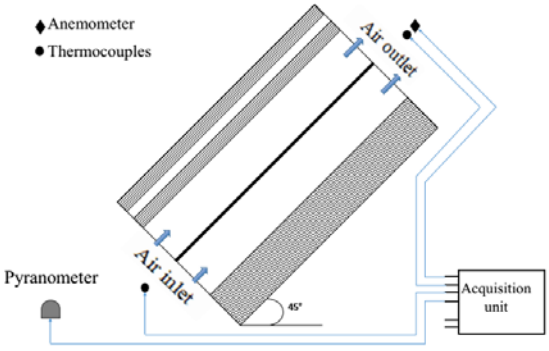

Fig. 3. Configuration for measuring the fluid temperatures at the inlet and outlet of the collector

2.3 Thermal performance evaluation

The power produced by the flow of energy from the sun (global power received, P_G) is obtained through the equation:

$$P_G = A \cdot G^* \tag{1}$$

where A is surface of upper glass cover (m^2) and G^* is solar radiation intensity (W/m^2).

The absorbed power, P_{ab} is expressed by the relation:

$$P_{ab} = \alpha \cdot \tau^2 \cdot A \cdot G^* \quad (2)$$

where α and τ are optical efficiency of the collector.

The thermal power received by the heat transfer fluid (useful power, P_u) passing through the collector is determined by the relation (Hu *et al.,* 2020; Ricci *et al.,* 2015):

$$P_u = \dot{m}\, c_p\, (T_s - T_e) \quad (3)$$

where $\dot{m}$ is air flow (kg/s).

The instantaneous overall efficiency of the collector, η is evaluated by the relation (Bahria *et al.*, 2013):

$$\eta = P_u / P_G \quad (4)$$

3. RESULTS AND DISCUSSION

3.1. Experimental characterization of the environment

The average monthly instantaneous evolution of solar radiation intensity (G* in W/m²) and ambient temperature are shown in Figure 4.

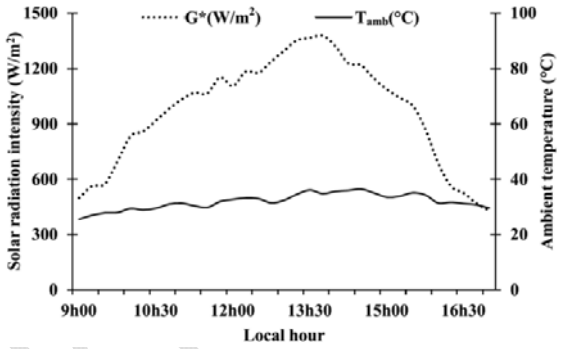

Fig. 4. Instantaneous evolution of solar radiation intensity and ambient temperature

This figure shows that the solar radiation intensity evolves in a bell shape, with a maximum value of around 1300±26 W/m². This result is in a good agreement with the numerical simulation made by Tetang and Ghiaus (2019). These solar flux values prove the sufficiency of solar irradiance for the performance evaluation of solar collectors since the American Society of Heating, Refrigerating and Air-Conditioning Engineers standard (ASHRAE) requires that for solar collector efficiency tests, solar irradiance must be above 630±12.6 W/m^2 (Abene *et al.,* 2004). Ambient temperature changes according to the amount of sunlight. The more sunlight, the more it increases. It's average value is 31.86±2 °C, which is higher than the annual average temperature in this zone, which is around 26±1°C (Tetang and Ghiaus, 2019). This can be translated by the fact that the month of April, in which the present work was carried out, is one of the hottest months of the year.

Figure 5 shows the evolution of relative humidity (RH) and wind velocity. Being subject to natural conditions, the air velocity is random and reaches a maximum value of 1.1 m/s. Relative humidity varies between 5 and 72%, with an uncertainty of ±1%. It continuously decreases from 9:00 am until 1:30 pm and increasing thereafter.

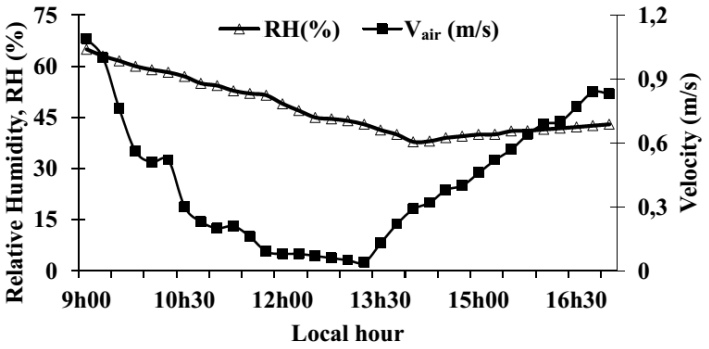

Fig. 5. Instantaneous evolution of relative humidity and air velocity

In this figure, we can see that between 9:30 and 14:00 (local time), the air speed decreases while the relative humidity also decreases. This means that the less humid the air is, the denser it is. Figure 5 also shows that the wind velocity profile at the site is highly variable. Its value remains below 0.5 m/s from 10:30 to 3:00 pm, therefore the need to use electrical fans in order to have a constant velocity regime inside the collector.

3.2. Experimental characterization of the collector

Figures 6, 7 and 8 show the temperature profiles of the absorber, the lower glass cover and the upper glass cover, respectively, correlated with the intensity evolution of solar radiation.

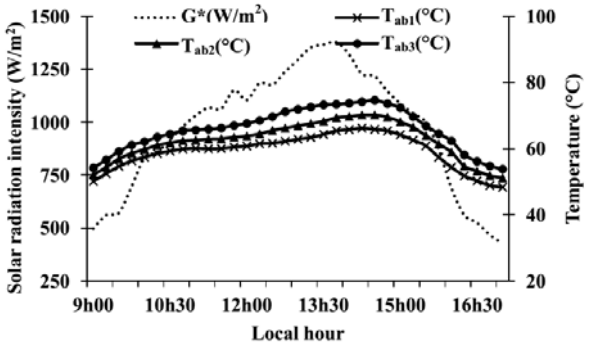

Fig. 6. Temperature profiles of the three measuring points of the absorber

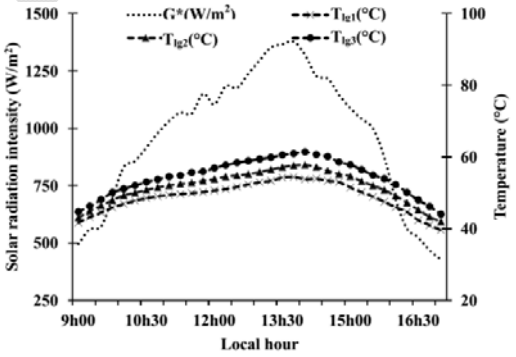

Fig. 7. Temperature profiles of the three measuring points on the lower glass cover

In Figures 6 and 7, the temperature profiles show a maximum temperature difference, between the outlet and the inlet of the collector, at 2:00 p.m. of 8.8 °C and 2.5 °C for the absorber and for the lower glass cover, respectively. This behavior can be explained by the heat exchange constraints that exist between the working fluid and the surface of these components. Indeed, the air being colder at the collector inlet heats up with the distance. Consequently the heat exchange between these components and the air is less intensive at the collector outlet.

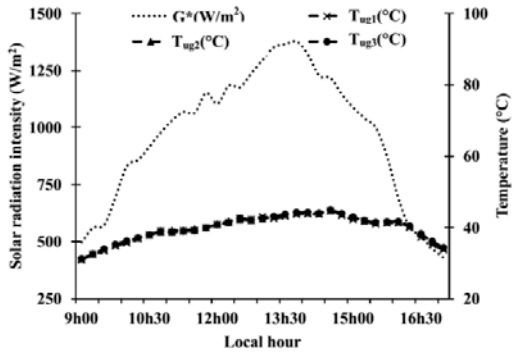

Fig. 8. Temperature profiles of the three measuring points on the upper glass cover

For the upper cover, the temperature profiles are practically identical for all three measuring points (Figure 8). The differences are around 0.3 °C, which can be assigned to the instrument or operator errors. This thermal behavior is explained by the fact that the entire upper cover is exposed to the ambient air, so that the different measuring points are subject to practically the same convective exchange conditions.

Figure 9 shows a comparison between the temperature profiles of the three main components of the collector at the third measuring point, at the output of the collector, the ambient temperature and the solar irradiance.

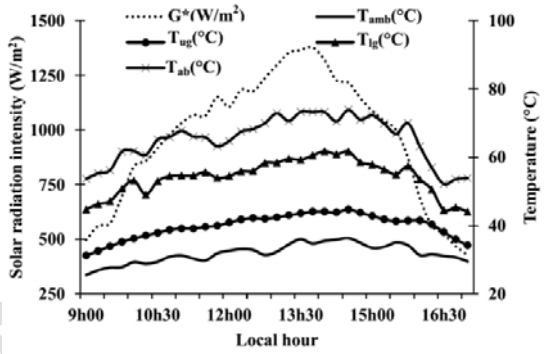

Fig. 9. Temperature profiles of the absorber and the upper and lower glass cover

This figure shows that the local temperatures are increasing from the outside to the inside of the collector. The absorber reaches its maximum temperature of 73.9 °C at 2:30 pm, when solar irradiance is 1217±24 W/m^2 and the ambient temperature has 35 °C. This temperature value shows that the absorber has a high absorption coefficient. Similar results were also obtained by Fouakeu *et al.,* (2019). The temperature has all the times higher values for the lower glass cover than for the upper cover and goes up to 61.7 °C and 44.7 °C, respectively, at 2:30 pm, with an uncertainty of ±2°C.

The following Figure 10 shows the outlet temperature profiles of the heat transfer fluid when it circulates at velocity of 0.5 m/s and 1.5 m/s, in comparison with the inlet temperature profile of the heat transfer fluid (ambient temperature).

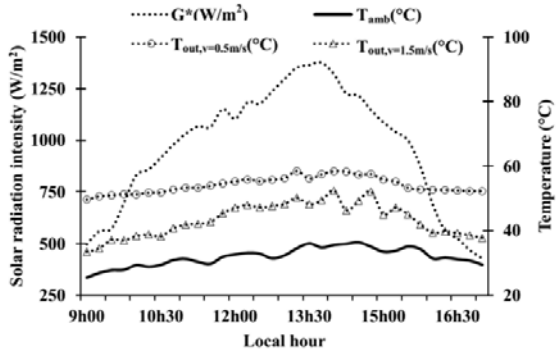

Fig. 10. Profiles of air inlet and outlet temperature

Regardless of the flow velocity, there is a considerable difference in the temperature of the heat transfer fluid between the outlet and inlet of the collector. This difference is around 22.4 °C when the velocity is 0.5 m/s, and 15.1 °C when the velocity is 1.5 m/s. The output temperatures are between 49.7 °C and 58.4 °C in the first case (0.5 m/s) and between 33.5 °C and 52.2 °C in the second case (1.5 m/s). The highest output values of temperature are registered at 1:15 pm for both velocity levels. This difference is explained by a longer residence time of the fluid in the collector when its velocity is 0.5 m/s. These results are in agreement with those found in the literature such as that of Semmar *et al.,* (1998) who had worked on the study and design of a solar air collector intended for the production of hot air. At the end of the work, they concluded that for higher velocity, there is a significant increase of heat flow despite the outlet temperature which is lower than that obtained for lower speeds where the heat flow is below the first one.

The following Figure 11 shows the evolution of the instantaneous global efficiency of the collector.

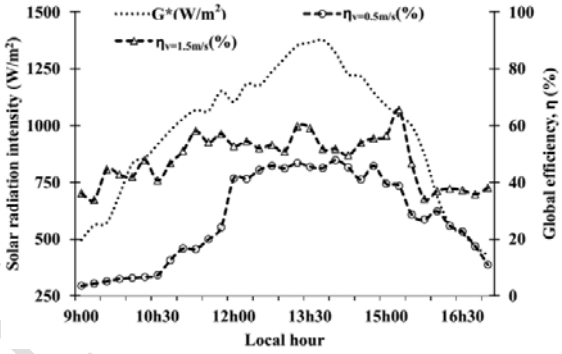

Fig. 11. Evolution of the instantaneous global efficiency

This figure shows that the instantaneous global efficiency of the collector has an average value of 27.38% when the air velocity is 0.5 m/s and 48.13% for the velocity of 1.5 m/s. This means that almost half of the energy produced by the sunlight on the collector is transmitted to the heat transfer fluid in the latter case. This result is in line with the work of Tetang and Ghiaus (2019) which shows that by varying the speed of the fluid, the efficiency also evolves according to the same profile, up to a certain threshold. The instantaneous global efficiency obtained in this study ranged from 20 to 79%, a range presented by Fudholi and Sopian (2019). This configuration of double pass and glass of solar collector has a better performance, compared to the configuration used by Hu *et al.,* (2020).

4. CONCLUSION

This work was focused on the experimental characterization of a double air pass solar collector. It was a solar collector realized to be coupled to a dryer for the conservation of fruits and vegetables. For this, it was a question of working in laminar regime. The experiments carried out revealed the influence of the flow velocity of the heat transfer fluid on its outlet temperature. It appears that the outlet temperatures of the heat transfer fluid are 58.4 °C and 52.2 °C for the air velocities of 0.5 m/s and 1.5 m/s, respectively. The global efficiency is up to 47.81% and 65.57% for a collector surface of

0.47 m². The results obtained show that this sensor configuration can be used with satisfaction, for the production of the heat necessary for drying in a humid tropical environment.

REFERENCES

Abene A, Dubois V, Le Ray M, Ouagued A. Study of a solar air flat plate collector: use of obstacles and application for the drying of grape, Journal of Food Engineering, 2004. 65, pp. 15–22.

Agbossou K, Tetang FA, Boroze TE, N'wuitcha K, Napo K, Zeghmati B. Theoretical and Experimental Study of Thermal Performance of Flat Plate Air Heating Collector. International Journal of Science and Technology, 2016. ISSN 2049-7318. Volume 5, N° 10, pp. 473-490.

Ahmed-Zaid A, Messaoudi H, Abenne A, Le Ray M, Desmons JY, Abed B. Experimental study of thermal performance Improvement of a solar air flat plate collector Through the use of obstacles: Application for the drying of yellow onion. International Journal of Energy Research, 1999. vol. 23, pp. 1083-1099.

Aoues K, Moummi N, Zellouf M, Moummi A, Labed A, Achouri E, Benchabane A. Amélioration des performances thermiques d'un capteur solaire plan à air : Etude expérimentale dans la région de Biskra. Revue des Energies Renouvelables, 2009. Vol. 12 N°2, pp. 237–248

Bahria S, and Amirat M. Influence de l'adjonction des chicanes longitudinales sur les performances d'un capteur solaire plan à air. Revue des énergies renouvelables, 2013. Vol. 16 N°1, pp. 51–63.

Dountio E, Guemene, Njomo D, Efa F, Simo A. On the reliability of HELIOSAT method: A comparison with experimental data. Solar Energy, 2010. 84. pp. 1047-1058.

Floride G, Tassou S, Kalogirou S, Wrobel L. Review of solar and low energy cooling technologies for buildings. Renewable Sustainable Energy Rev., 2002. 6(6), pp. 557-572.

Fouakeu NGA, Tetang FA, Edoun M, Kuitche A, Zeghmati B, A contribution to a numerical characterization of the thermal transfers in a saw tooth solar collector. International Journal of Thermal Technologies, 2019. E-ISSN 2277 – 4114, Vol.9, N°3, pp. 200-206. DOI: 10.14741/ijtt/v.9.3.1.

Fudholi A, and Sopian K. A review of solar air flat plate collector for drying application. Renewable and Sustainable Energy Reviews. 2019, 102, pp. 333–345.

Gorjian S, Ebadi H, Calise F, Shukla A, Ingrao C. A review on recent advancements in performance enhancement techniques for low-temperature solar collectors. Energy Conversion and Management. 2020. 222, 113246.

Hu J, Guo M, Guo J, Zhang G, Zhang Y. Numeric al and experimental investigation of solar air collector with internal swirling flow. Renewable Energy, 2020. 162, pp. 2259-2271.

Ihaddadene R, Ihaddadene N, Mahdi A. Effect of Distance between Double Glazing on the performance of a Solar Thermal Collector, in Editor: Book Effect of distance between double glazing on the performance of a solar thermal collector, 2014. 5 p.

Kalogirou S, Design, construction, performance evaluation, and economic analysis of an integrated collector storage system. Renewable Energy, 1997. 12(2), pp. 179-192.

Labed A, Moummi N, and Benchabane A. Experimental investigation of various designs of solar flat plate collectors: Application for the drying of green chili, Journal of Renewable and Sustainable Energy, 2012. vol. 4, 043116.

Labed A, Moummi N, Aouès K, Zellouf M, Moummi A. Etude théorique et expérimentale des performances d'un capteur solaire plan à air muni d'une nouvelle forme de rugosité artificielle. Revue des Energies Renouvelables, 2009. Vol. 12, N°4, pp. 551–561.

Mahmut SB, Saffa BR. Building integrated solar thermal collectors – A review. Renewable and Sustainable Energy Reviews, 2015. 51; pp. 327-346.

Mokhtari F and Semmar D. L'influence de la configuration de l'absorbeur sur les performances thermiques d'un capteur solaire à air. Revue des Energies Renouvelables : Journées de Thermique, 2001. pp. 159-162.

Ricci M, Bocci E, Michelangeli E, Micangeli A, Villarini M, Naso V. Experimental tests of solar collectors prototypes systems. Energy Procedia. 2015. 82, pp. 744-751.

Semmar D, Betrouni S, and Lafri D. Etude et réalisation d'un capteur solaire à air. Revue des Energies Renouvelables : Physique Energétique, 1998. pp. 33–38.

Suman S, Kaleem KM, Pathak M. Performance enhancement of solar collectors— A review. Renewable and Sustainable Energy Reviews. 2015. 49, 192–210.

Tetang FA and Ghiaus A-G. Influence of geometric parameters on the thermal performances of a double air pass solar collector. Science Journal of Energy Engineering. 2019. Vol. 7, No. 4, pp. 67-76. DOI: 10.11648/j.sjee.20190704.13.